

parameter away. Thus,

$$\Delta E_2 = 2\Delta E_m. \quad (51)$$

Taking the average $\delta E + \Delta E$ per jump, we find

$$\delta E + \Delta E = \frac{1}{2}(\delta E_1 + \delta E_2 + \Delta E_1 + \Delta E_2). \quad (52)$$

$$\delta E + \Delta E = \Delta E_m + \Delta E_f + kTad(\ln \gamma_i)/dx. \quad (53)$$

Ignoring correlation,

$$\delta E + \Delta E = -kTa \left[\frac{1}{D_i^*} \frac{dD_i^*}{dx} - \frac{d \ln \gamma_i}{dx} \right]. \quad (54)$$

Now, for interstitial diffusion, $D^* = a^2\nu$, where ν is the frequency of tracer jumps in a given direction when successive lattice-to-interstitial and interstitial-to-lattice jumps are counted as separate jumps. Hence the final expression for the shift in center of gravity is the same as for the vacancy or interstitial mechanisms if the terms due to correlation and flow of imperfections are neglected. Also, it can be shown that there will be no net effect from correlation on the shift in center of gravity, the situation being similar to that for a vacancy mechanism where the correlation term in Eq. (13) exactly cancelled that in Eq. (26).

Theory of Nuclear Spin Relaxation in Superconductors

L. C. HEBEL

Bell Telephone Laboratories, Murray Hill, New Jersey

(Received May 13, 1959)

Using analytical methods, a new evaluation has been made of R_s/R_n , the ratio of nuclear spin-lattice relaxation rate in the superconducting phase to that in the normal phase, from expressions previously derived by Hebel and Slichter using the Bardeen-Cooper-Schrieffer theory of superconductivity. The results are given for several values of the effective breadth of the Bardeen-Cooper-Schrieffer energy levels.

SEVERAL measurements of nuclear spin-lattice relaxation in normal and superconducting aluminum¹⁻³ have been reported recently. Hebel and Slichter² discuss the theory of the spin-lattice relaxation rates, R_s and R_n , in superconducting and normal phases, respectively, and they give curves of R_s/R_n versus temperature calculated using the Bardeen-Cooper-Schrieffer (BCS) theory⁴ of superconductivity. This article presents an improved calculation of R_s/R_n based on the discussion of Hebel and Slichter.²

In thermal equilibrium the nuclear spin level populations are determined by a Boltzmann distribution characterized by the lattice temperature. The nuclear spin-lattice relaxation rate, R , is defined as the characteristic rate of approach to such a thermal equilibrium situation from a nonequilibrium one. In a metal the nuclear magnetic moments have a strong magnetic interaction with the moments of the conduction electrons, which are in very good contact with the lattice. Consequently, in a metal the scattering of nuclear spins by conduction electron spins determines R , since such scattering provides the fastest means of the nuclei achieving thermal equilibrium with the lattice. Hebel and Slichter calculate how superconductivity affects

R using the BCS theory to treat the conduction electrons.

The equation which they obtain for R_s/R_n is given in terms of the following quantities: the first is the normalized density of electron states in the superconductor, $\rho_s(E, T)$, which from BCS theory has a temperature-dependent gap of half-width $\epsilon_0(T)$ centered about the Fermi energy, E_F ; the second is Δ , the effective energy breadth of the BCS states; the third quantity is the Fermi distribution function, $f(E, T)$. In terms of $x = (E - E_F)/kT$, $\delta = \Delta/kT$, and $\eta_0(T) = \epsilon_0(T)/kT$, Hebel and Slichter² show that

$$R_s/R_n = 2 \int_0^\infty \rho_s^2(x, T) [1 + \eta_0^2(T)/x^2] \times f(x, T) [1 - f(x, T)] dx. \quad (1)$$

The density of states, ρ_s , is obtained by weighting the BCS density of states, ρ_{BCS} , with the function which characterizes the breadth of the energy levels. If an energy level breadth function is used which is a rectangle of width 2Δ and height $1/2\Delta$, then

$$\rho_s(x, T) = (2\delta)^{-1} \int_{-\delta}^{x+\delta} \rho_{BCS}(y, T) dy, \quad (2)$$

where

$$\rho_{BCS}(y, T) = 0, \quad |y| < \eta_0, \quad (3a)$$

$$\rho_{BCS}(y, T) = [y^2/(y^2 - \eta_0^2(T))]^{\frac{1}{2}}, \quad |y| > \eta_0. \quad (3b)$$

¹ L. C. Hebel and C. P. Slichter, Phys. Rev. **107**, 901 (1957).

² L. C. Hebel and C. P. Slichter, Phys. Rev. **113**, 1504 (1959).

³ A. G. Anderson and A. G. Redfield, Bull. Am. Phys. Soc. **2**, 388 (1957); A. G. Redfield, Physica **24**, 5150 (1958); A. G. Redfield, Phys. Rev. Letters **3**, 85 (1959).

⁴ Bardeen, Cooper, and Schrieffer, Phys. Rev. **108**, 1175 (1957).

TABLE I. R_s/R_n versus η_0 for various values of $r = \epsilon_0(0)/\Delta$ (the ratio of gap width to level breadth) using BCS theory to obtain T/T_c and T_c/T versus η_0 .

η_0	R_s/R_n for					From BCS	
	$r=15$	$r=60$	$r=200$	$r=600$	$r=2000$	T/T_c	T_c/T
0.50	1.56	2.03	2.31	2.57	2.85	0.973	1.027
0.70	1.78	2.35	2.73	3.07	3.44	0.950	1.053
1.00	1.97	2.59	3.07	3.50	3.97	0.9075	1.102
1.25	2.02	2.64	3.16	3.64	4.16	0.858	1.166
1.50	1.97	2.58	3.12	3.61	4.15	0.810	1.235
1.75	1.87	2.45	2.98	3.47	4.00	0.760	1.317
2.00	1.73	2.26	2.76	3.22	3.73	0.7125	1.403
2.50	1.38	1.79	2.22	2.60	3.02	0.625	1.600
3.00	1.03	1.33	1.66	1.96	2.28	0.547	1.828
3.50	0.741	0.948	1.19	1.41	1.65	0.482	2.075
4.50	0.350	0.442	0.559	0.667	0.785	0.382	2.615
6.00	0.102	0.126	0.162	0.194	0.230	0.290	3.45
9.00	0.00746	0.00878	0.0115	0.0139	0.0166	0.1945	5.14

Thus,

$$\rho_s = 0, \quad |x| \leq \eta_0 - \delta, \quad (4a)$$

$$\rho_s = (2\delta)^{-1} [(x+\delta)^2 - \eta_0^2]^{\frac{1}{2}}, \quad \eta_0 - \delta \leq |x| \leq \eta_0 + \delta, \quad (4b)$$

$$\rho_s = (2\delta)^{-1} \left\{ [(x+\delta)^2 - \eta_0^2]^{\frac{1}{2}} - [(x-\delta)^2 - \eta_0^2]^{\frac{1}{2}} \right\}, \quad |x| \geq \eta_0 + \delta. \quad (4c)$$

The level breadth is expected to be much less than the gap width. Consequently, one may break up R_s/R_n into two integrals, I_1 and I_2 , by introducing a parameter β such that $1 \gg \beta \gg \delta/\eta_0$. In I_1 , where $|x| \leq \beta\eta_0$, $f(x)[1 - f(x)]$ may be taken outside the integral; in I_2 , where $|x| \geq \beta\eta_0$, ρ_s may be set equal to ρ_{BCS} . Using

$$4f(x)[1 - f(x)] = \text{sech}^2(\frac{1}{2}x), \quad (5)$$

one obtains for I_1 ,

$$I_1 = \frac{1}{2}\eta_0 \text{sech}^2(\frac{1}{2}\eta_0) \left\{ 1 + (\beta\eta_0/\delta)^2 - (\beta\eta_0/\delta) [(\beta\eta_0/\delta)^2 - 1]^{\frac{1}{2}} + \ln((\beta\eta_0/\delta) + [(\beta\eta_0/\delta)^2 - 1]^{\frac{1}{2}}) \right\}. \quad (6)$$

For most cases of interest

$$\frac{2\beta\eta_0}{\delta} = \left[\frac{2\beta\epsilon_0(0)}{\Delta} \right] \frac{\epsilon_0(T)}{\epsilon_0(0)} \gg 1;$$

thus, an expansion of Eq. (6) may be used.

$$I_1 \cong \frac{1}{2}\eta_0 \text{sech}^2(\frac{1}{2}\eta_0) \left[\frac{3}{2} + \frac{1}{2}(\delta/2\beta\eta_0)^2 + \ln(2\beta\eta_0/\delta - \delta/2\beta\eta_0) \right]. \quad (7)$$

Equation (7) was used to obtain the contribution of I_1 to the results for R_s/R_n tabulated in Table I and Fig. 1. The results are given in terms of $\epsilon_0(0)/\Delta$, the ratio of absolute zero gap width to energy level breadth. In Eq. (7), $\beta=0.05$ was used for $\epsilon_0(0)/\Delta=60, 200, 600, 2000$; $\beta=0.2$ was used for $\epsilon_0(0)/\Delta=15$.

I_2 cannot be evaluated exactly. It may be written

$$I_2 = \frac{1}{2} \int_{\eta_0(1+\beta)}^{\infty} \frac{x^2 + \eta_0^2}{x^2 - \eta_0^2} \text{sech}^2(\frac{1}{2}x) dx. \quad (8)$$

For small η_0 , I_2 can be evaluated to lowest order in η_0 , with the result,

$$I_2 \cong 1 + \frac{1}{2}\eta_0 \left\{ \ln \left[\frac{2}{\beta} + 1 \right] - (1 + \beta) \right\}, \quad \eta_0 \ll 1. \quad (9)$$

For large η_0 , another type of expansion may be used. Writing

$$I_2 = \int_a^b g(x)h(x)dx, \quad (10)$$

if $h(x)$, $xh(x)$, and $x^2h(x)$ are integrable, and if $g(x)$ is slowly varying, then one may expand $g(x)$ in a Taylor series and keep the lowest terms; in addition, suitable choice of expansion point eliminates the first order error term. By choosing

$$\bar{x} = \int_a^b xh(x)dx, \quad (11)$$

then

$$I_2 = g(\bar{x}) \int_a^b h(x)dx + \frac{1}{2} \frac{d^2g}{dx^2} \bigg|_{\bar{x}} \int_a^b (x-\bar{x})^2 h(x)dx + \dots \quad (12)$$

To have $g(x)$ slowly varying, we choose

$$g(x) = \frac{2(x^2 + \eta_0^2)}{(x + \eta_0)(1 + e^{-x})^2} \quad \text{and} \quad h(x) = \frac{e^{-x}}{x - \eta_0}. \quad (13)$$

Then,⁵

$$\int_a^b h(x)dx = e^{-\eta_0} \int_{\beta\eta_0}^{\infty} x^{-1} e^{-x} dx = e^{-\eta_0} \text{Ei}(\beta\eta_0), \quad (14)$$

and

$$\bar{x} = \int_a^b xh(x)dx = \eta_0 \left[1 + \frac{e^{-\beta\eta_0}}{\eta_0 \text{Ei}(\beta\eta_0)} \right]. \quad (15)$$

For large enough η_0 , the slowly varying character of

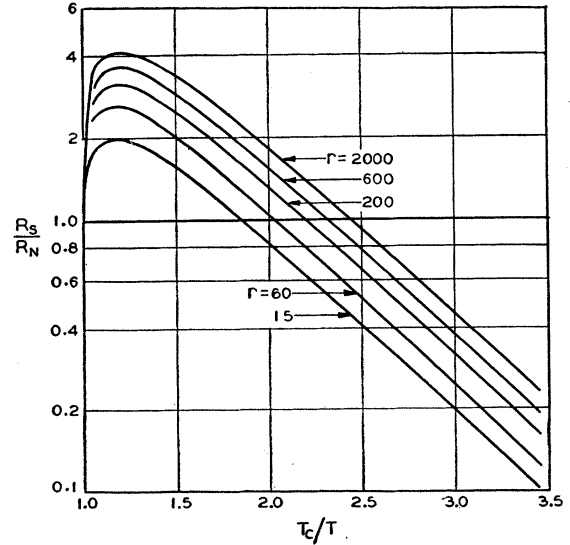


FIG. 1. R_s/R_n versus T_c/T for various values of $r = \epsilon_0(0)/\Delta$.

⁵ E. Jahnke and F. Emde, *Tables of Functions* (Dover Publications, New York, 1943).

$g(x)$ causes the second order term in Eq. (12) to be small, so that for η_0 sufficiently large,

$$I_2 \cong \frac{2(\bar{x}^2 + \eta_0^2)e^{-\eta_0} \text{Ei}(\beta\eta_0)}{(\bar{x} + \eta_0)[1 + \exp(-\bar{x})]^2} \quad (16)$$

The values of I_2 versus η_0 are needed for $\beta=0.05$ and $\beta=0.2$. A connecting function is needed for each value of β to connect the expression for I_2 in Eq. (9), valid for small η_0 , with that in Eq. (16), valid for sufficiently large η_0 . The function

$$I_2 = \frac{(1+C)e^{\frac{1}{2}(a-b)\eta_0}}{1+Ce^{-\frac{1}{2}b\eta_0}}$$

connects the points and slopes to within 1% using the following parameters: for $\beta=0.05$, $C=2.380$, $b=5.560$, and $a=4.305$; for $\beta=0.2$, $C=1.735$, $b=4.72$, and $a=2.93$. Investigation of the second order error term in Eq. (12) for I_2 shows that I_2 is represented by its asymptotic form, Eq. (16), to better than 2% for $\eta_0 \geq 1.50$ for both values of β .

The relation between $\eta_0 = \epsilon_0(T)/kT$ and temperature, which was used in compiling Table I, was taken from BCS theory using their temperature dependence of $\epsilon_0(T)$ and $\epsilon_0(0) = 3.5kT_c$. A change in either factor would change only the temperature scale of Table I and Fig. 1, since all calculations scale as η_0 itself (i.e., —only the values of η_0 themselves appear in the equation). Thus, the results in Table I may easily be extended to the case of an experimental gap width by using the new relation between η_0 and temperature. One should note that the value of $\epsilon_0(0)/\Delta$ assigned to the table might also be changed. The energy level breadth, Δ , was assumed to be independent of temperature. [Such an assumption allows Δ to be interpreted also as an anisotropy in $\epsilon_0(0)$ in k space.] The effect of a temperature dependent Δ can be obtained by moving from one value of $\epsilon_0(0)/\Delta$ to another in changing temperature.

ACKNOWLEDGMENTS

The author wishes to thank Dr. M. Lax for several suggestions concerning suitable approximation methods for I_2 .

Origin of the Characteristic Electron Energy Losses in Magnesium*

C. J. POWELL AND J. B. SWAN

Department of Physics, University of Western Australia, Nedlands, Western Australia

(Received May 12, 1959)

The characteristic electron energy loss spectrum of magnesium has been measured by analyzing the energy distribution of 750-, 1000-, 1505-, and 2020-ev electrons scattered by an evaporated specimen through 90°. The spectra were similar in form to those previously obtained with aluminum targets, in that the observed loss peaks were composed entirely of combinations of two elementary energy losses. These two losses, of magnitude 7.1 and 10.6 ev, were identified, respectively, with the lowered plasma loss proposed by Ritchie and the plasma loss proposed by Bohm and Pines.

INTRODUCTION

IN a previous paper,¹ the origin of the characteristic electron energy losses in aluminum was discussed in some detail. It was shown there that the characteristic loss spectrum of aluminum is made up of combinations of elementary 10.3- and 15.3-ev losses, the former, the low-lying loss, being identified with the lowered plasma loss proposed by Ritchie,² and the latter with the plasma loss proposed by Bohm and Pines.³

The characteristic loss spectrum of magnesium has

been studied by a number of workers,⁴⁻¹¹ and the observed loss values are shown in Table I. The shape of the magnesium spectrum has been found to be similar to that of aluminum, in that a sharp energy loss is observed, together with one or more lines due to multiples of this elementary loss. This sharp line, occurring at ~10 ev in magnesium, has generally been regarded as arising from collective electron excitation³

⁴ L. Marton and L. B. Leder, Phys. Rev. **94**, 203 (1954).

⁵ L. B. Leder and L. Marton, Phys. Rev. **95**, 1345 (1954).

⁶ H. Watanabe, J. Phys. Soc. Japan **9**, 1035 (1954).

⁷ W. Kleinn, Optik **11**, 226 (1954).

⁸ Blackstock, Ritchie, and Birkhoff, Phys. Rev. **100**, 1078 (1955).

⁹ G. W. Jull, Proc. Phys. Soc. (London) **B69**, 1237 (1956).

¹⁰ V. I. Milyutin and A. I. Kabanov, Uspekhi Fiz. Nauk. **61**, 673 (1957).

¹¹ N. B. Gornyi, Izvest. Akad. Nauk. S.S.S.R. Ser. Fiz. **22**, 475 (1958).

* Work supported by the Research Grants Committee of the University of Western Australia.

¹ C. J. Powell and J. B. Swan, Phys. Rev. **115**, 869 (1959).

² R. H. Ritchie, Phys. Rev. **106**, 874 (1957).

³ D. Pines and D. Bohm, Phys. Rev. **85**, 338 (1952); D. Pines, Revs. Modern Phys. **28**, 184 (1956); P. Nozières and D. Pines, Phys. Rev. **109**, 1062 (1958).